Progress In Electromagnetics Research C, Vol. 149, 155-163, 2024 PIER C

(Received 6 September 2024, Accepted 30 October 2024, Scheduled 2 November 2024)

Design a Dual-Band with CSRR Cascaded Patch Antenna Array for Wireless Communications

Maloth Chandrasekhar[1] and Ketavath Kumar Naik[2,*]

[1]Department of ECE, KITS (A) Warangal, Telangana, India
[2]Department of Electronics and Communication Engineering
Koneru Lakshmaiah Education Foundation (KLEF) deemed to be University, Vaddeswaram, Guntur 522502, India

ABSTRACT: This paper presents a dual-band cascaded rectangular microstrip patch antenna array with a complementary split ring resonator (CSRR) for narrow-band wireless communication applications. The antenna array is fed with a microstrip feed line for proper impedance matching, and CSRR is loaded to generate dual-band characteristics. The CSRR-based proposed antenna radiators operate over two frequency bands, i.e., 100 MHz (3.06–3.16 GHz) and 110 MHz (4.36–4.47 GHz) with reflection coefficients ($S_{11} < -10$ dB) of -23 dB and -32 dB. The gain of the proposed antenna array with CSRR is 5.03 dBi and 6.34 dBi at 3.1 GHz and 4.4 GHz, respectively. In addition, S-parameters, radiation patterns, 3D gain characteristics, and surface current distribution at resonating frequencies are observed. The proposed antenna array is miniaturized in size and suitable for wireless communication applications.

1. INTRODUCTION

Nowadays it is being practiced to develop dual or multi-functional designs. The motive is to diminish the framework size and cut the framework cost. Microstrip array antennas have interesting qualities like system capacities and gains with high levels. The cascaded antenna array's high gain characteristics made the wide usage of Wireless Fidelity [1] and Worldwide Interoperability for Microwave Access communication [2] possible. Along with this, some challenges are faced inside the array in larger antenna sizes, mutual coupling effect, gain, and narrow bandwidths for wireless applications. Common microstrip patch antennas are less rated than array antennas. The growing technologies in wireless communication applications of base stations are trying to lower the number of antennas and improve the effectiveness of remote frameworks wireless systems. This requires the array antennas with high gain [3] and linear polarization [4]. An antenna with dual-polarizations and electromagnetic feeds [5] improved the impedance bandwidth of the return loss. Vertical polarization was achieved using an L-shaped electric probe, while horizontal polarization was attained through a magnetic loop. To improve the wide bandwidths, a rectangular patch antenna with dual-polarization was excited by two coax-line feeds [6] for linearly polarized array antennas [7] with multiple-layer substrates used. The use of multi-layer substrates may lead to advanced complex fabrications and high capacitive loss in array antennas [8]. Reducing the antenna's size, as indicated in [9], while simultaneously enhancing the bandwidth, as referenced in [10], is not feasible. To achieve wider bandwidth [11], perforated [12] or fractal arrays [13] are employed [14], as noted in [15], However, in the desired range of frequency, the gain radiation is not relevant [16]. The isolation of dielectric resonating antenna [17] is around 15 dB whereas cutting the array becomes one of the big challenges.

The dual-band applications [18] with defected ground structure (DGS) use circular patches [19]. Two concentric ring openings with DGS [20] are used for intensifying gain and bandwidths. A CPW-fed [21], monopole broadband antenna is suggested for giving rise to new modes of resonance by matching fine impedance including antenna operations on communication bands [22] for improving the bandwidths [23], and different configurations of U-shaped slots are etched from the designs [24]. For metal-insulator-metal (MIM) multiple-input multiple-output (MIMO)-specific absorption rate (SAR) applications [25], a compact dual-band dual-polarized (DBDP) microstrip antenna array with dimensions of $77 \times 79 \times 2.2\,\text{mm}^3$ is introduced. For wireless communication [26], a dual-polarized antenna array [27] with conical factors was put forth [28]. A linearly polarized antenna [29] has superior coverage compared to that is circularly polarized [30]. A crescent-shaped slot [31] antenna is proposed for wireless [32] and internet of things (IoT) applications [33]. An optical [34] triangle-shaped [35] monopole antenna was proposed for wireless applications [36]. Micro-electromechanical system (MEMS) antennas [37] are also used for telecommunication [38] wireless applications. A periodic antenna [39], utilizing CPW feeding technique [40], offered improved antenna properties [41] suitable for wireless communication [42].

2. ANTENNA STRUCTURE

The top view and bottom view of the dual-band cascaded rectangular microstrip patch antenna array with a complementary split ring resonator (CSRR) are shown in Figs. 1(a) and (b).

* Corresponding author: Ketavath Kumar Naik (drkumarkn@hotmail.com).

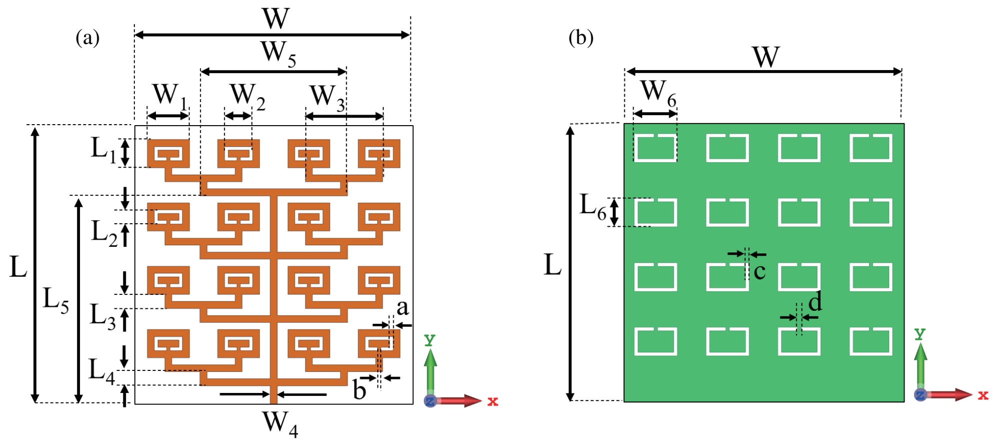

FIGURE 1. Physical structure of proposed antenna. (a) Top view. (b) Bottom view.

TABLE 1. Optimum values of design parameters.

Parameters	Value (mm)	Parameters	Value (mm)	Parameters	Value (mm)
L	40	L_5	30	W_5	21
W	40	L_6	4	W_6	6
L_1	4	W_1	6	a	0.5
L_2	2	W_2	4	b	0.5
L_3	2	W_3	11	c	0.5
L_4	2	W_4	1	d	0.5

Low-cost FR-4 substrate material is used to design the proposed antenna prototype with dimensions of $L \times W \times t\,\text{mm}^3$. The thickness of the substrate is denoted as 't', and its value is 1.6 mm. The proposed substrate material has a loss tangent of 0.02 and a dielectric constant of 4.4. A microstrip feed line structure is proposed for 50-ohm impedance matching. The dimensions of the microstrip feed line are $1 \times 30\,\text{mm}^2$ along the X- and Y-axes. Table 1 shows the optimum dimensional values for each parameter utilized in the design process of the proposed antenna. Figs. 1(a) and (b) show the physical structure and detailed dimensions of the proposed antenna. In this paper, the radiating patch is coated on one side of the substrate, and the ground plane is coated on the other side of the substrate. Rectangular CSRRs on both the patch and ground plane are used to resonate the dual bands for the proposed antenna at the required resonating frequencies.

From Figs. 1(a) and (b), the slot width of the rectangular CSRR of patch and ground plane is 'a' and 'c'. The length and width of the CSRR on the patch are $L_2 \times W_2$ along the X- and Y-axes. Further, the cascaded array of rectangular radiator patch dimensions is $L_1 \times W_1$ along the X-axis and Y-axis, respectively. The spacing between the array elements is W_5 whose value is shown in Table 1. All the design antenna parameters are optimized using the CMA (Covariance matrix adaptation) algorithm. All the radiating elements and ground planes are designed using 0.01 mm thick copper material and are considered perfect conductors during analysis.

Table 1 shows the optimized parametric values of the proposed antenna array. Equations (1) and (2) are utilized to calculate the physical dimensions of the proposed basic rectangular patch antenna [9].

$$W = \frac{C}{2f_r}\sqrt{\frac{2}{\varepsilon_r+1}} \tag{1}$$

$$L = \left\{\frac{C}{2f_r\sqrt{\varepsilon_{reff}}}\right\} \tag{2}$$

The effective dielectric constant, ε_{reff}, is calculated as:

$$\varepsilon_{reff} = \frac{\varepsilon_r+1}{2} + \frac{\varepsilon_r-1}{2}\left[\left(1+\frac{12t}{W}\right)^{-\frac{1}{2}} + 0.04\left(1-\frac{W}{t}\right)^2\right] \tag{3}$$

where C is the velocity of light, ε_r the relative dielectric constant, t the thickness of the substrate, and f_r the resonant frequency.

3. DESIGN AND ANALYSIS OF CASCADED ANTENNA ARRAY

3.1. Design Process of Proposed Antenna

The evaluation process of the proposed antenna array is explained in four steps as shown in Figs. 2(a)–(d). Initially, in the first step, a plain rectangular cascaded antenna array with a conventional ground plane structure is considered as Ant. 1 shown in Fig. 2(a). Ant. 1 resonates at 3.2 GHz frequency with

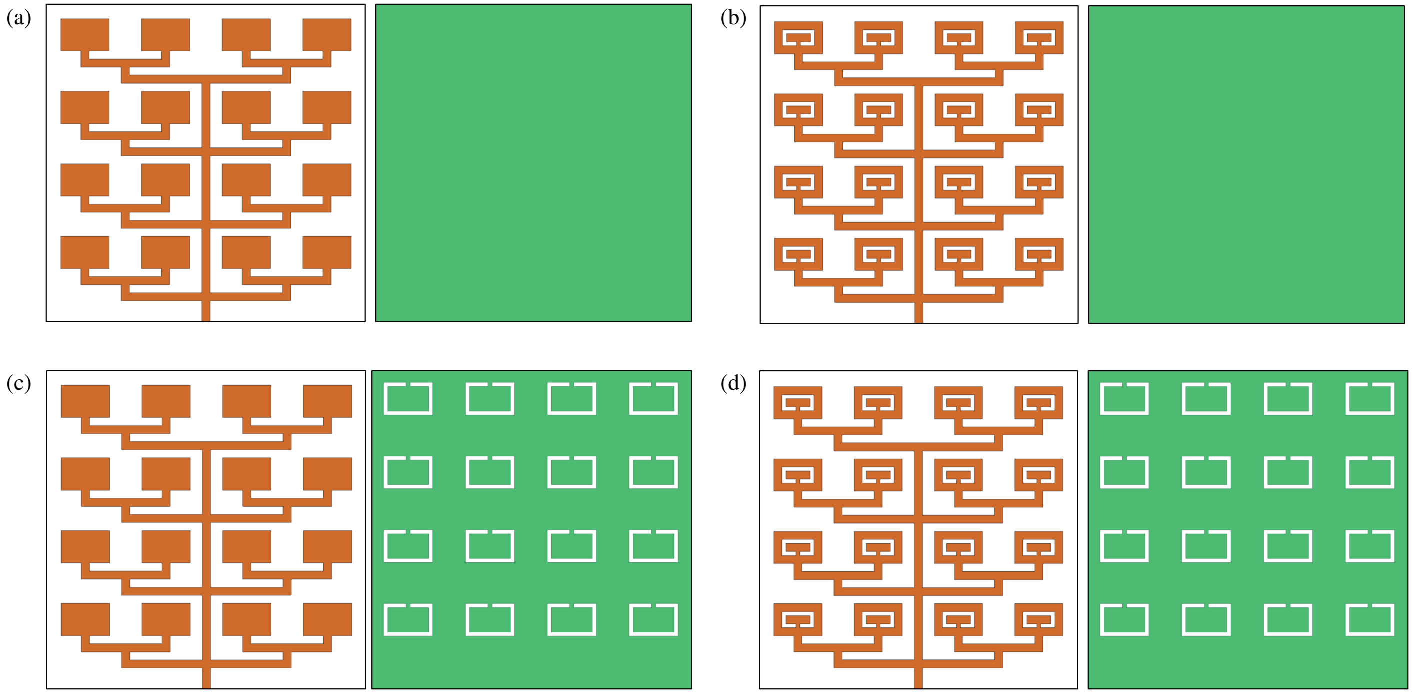

FIGURE 2. Evolution process of array. (a) Ant. 1, (b) Ant. 2, (c) Ant. 3, (d) Ant. 4.

a reflection coefficient of −14 dB. Ant. 1 has a minimum bandwidth of 50 MHz and a low gain of 1.84 dBi. Hence, to improve the bandwidth and gain characteristics, Ant. 2 is designed in the second step. The complementary split ring resonators are etched from the cascaded rectangular array along with complete ground plane, and it is considered as Ant. 2 shown in Fig. 2(b). Ant. 2 resonates at 3.3 GHz with a return loss of −22 dB. The bandwidth and gain of Ant. 2 are 60 MHz and 2.14 dBi. Furthermore, to produce dual-band characteristics, Ant. 3 is considered. In the next step, a complementary split ring resonator (CSRR) is etched from the ground plane, and the patch remains constant like Ant. 1 and is called Ant. 3 shown in Fig. 2(c). Ant. 3 resonates at 3.0 GHz and 4.3 GHz frequencies with reflection coefficients of −15 dB and −23 dB, respectively. Also, Ant. 3 has gain and bandwidth of 3.28 dBi, 4.86 dBi, 50 MHz, and 70 MHz at operating frequencies, respectively. Ant. 3 produces dual-band characteristics; however, the bandwidth and gain values are not enough for the required application. Hence, to enhance the antenna parameters like return loss, gain, and bandwidth, Ant. 4 (proposed) is considered.

Antenna 4 (Ant. 4) is designed by etching CSRRs on both the radiating cascaded patch array and the ground plane to achieve the desired characteristics illustrated in Fig. 2(d). Ant. 4 resonates at 3.1 GHz and 4.4 GHz frequencies with reflection coefficients of −23 dB and −32 dB, respectively. Also, Ant. 4 has gain and bandwidth of 5.03 dBi, 6.34 dBi, 100 MHz, and 110 MHz at operating frequencies, respectively. Fig. 3 shows the evolution processes of the proposed cascaded array antenna concerning the characteristics of the reflection coefficient, and its quantitative analysis is shown in Table 2.

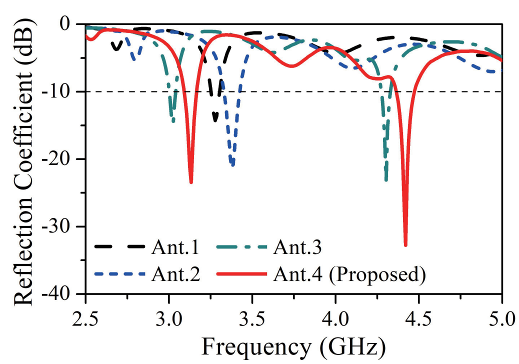

FIGURE 3. Designing process of the proposed antenna for reflection coefficient.

3.2. Parametric Analysis

The parametric analysis has been used to understand how a proposed antenna design evolved through various steps. The performance of the proposed dual-band antenna has been evaluated using CST Microwave Studio [43]. The antenna characteristics of resonant frequency, reflection coefficient, and bandwidth are more of a concern in this paper. The proposed design process incorporates approximately 18 parameters. The effects of all parameters are analyzed, but for brevity, we have only presented some of them. The parameters L_1, W_1, L_4, and W_4 are considered. The dimensions of the rectangular patch in the proposed array are $L_1 \times W_1$, as shown in Fig. 1(a). L_1 is varied from 3 mm to 5 mm with a step size of 1 mm to obtain the optimum value of the parameter. In Fig. 4(a), the impact of parameter L_1 is explained. The antenna has its lowest return-loss response when L_1 is 3 mm. When L_1 is 4 mm, the antenna's bandwidth and reflection coefficient are improved. Further in-

TABLE 2. Comparison of the proposed antenna array for design steps.

Iteration	operating frequency (GHz)	Frequency band (GHz)	Bandwidth (MHz)	Gain (dBi)	Reflection Coefficient (dB)
Ant-1	3.2	3.25–3.30	50	1.84	−14
Ant-2	3.3	3.30–3.36	60	2.14	−22
Ant-3	3.0	2.98–3.03	50	3.28	−15
	4.3	4.30–4.37	70	4.86	−23
Ant-4 (Proposed)	3.1	3.06–3.16	100	5.03	−23
	4.4	4.36–4.47	110	6.34	−32

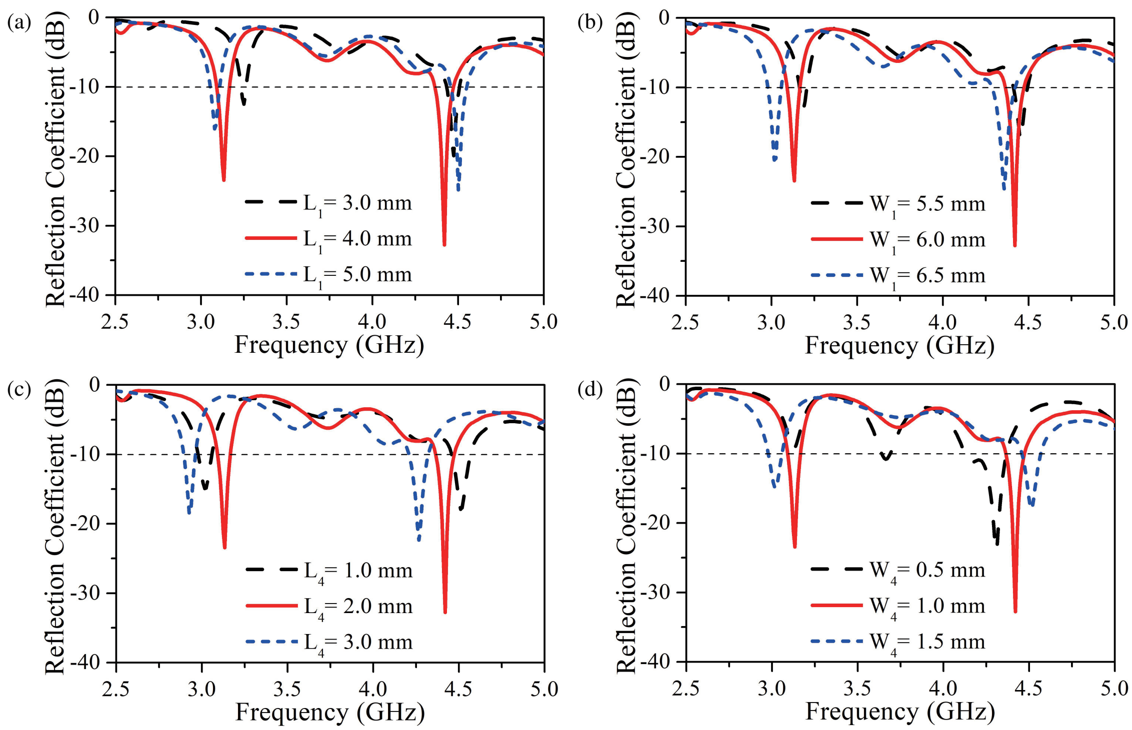

FIGURE 4. Parametric analysis of proposed antenna. (a) Parameter L_1. (b) Parameter W_1. (c) Parameter L_4. (d) Parameter W_4.

crease of L_1 is 5 mm; the return loss response and bandwidth are low. Hence, the optimum value of L_1 is 4 mm. Similarly, the parametric effect W_1 is explained in Fig. 4(b). It varies from 5.5 mm to 6.5 mm, with a step size of 0.5 mm. The bandwidth and return loss of the antenna are low when W_1 is 5.5 mm and 6.5 mm. However, the reflection coefficient and bandwidth value are improved when W_1 is 6 mm. Therefore, the optimum result is obtained at $W_1 = 6$ mm for the proposed antenna.

The length and width of the microstrip feed line in the proposed antenna array are $L_4 \times W_4$, as shown in Fig. 1(a). L_4 is varied from 1 mm to 3 mm with a step size of 1 mm to obtain the optimum value of the parameter. In Fig. 4(c), the impact of parameter L_4 is explained. The antenna has its lowest return-loss response when L_4 is 1 mm. When L_4 is 2 mm, the antenna's bandwidth and reflection coefficient are improved. Further increase of L_4 is 3 mm; the return loss response and bandwidth are low. Hence, the optimum value of L_4 is 2 mm. Similarly, the parametric effect W_4 is explained in Fig. 4(d). It varies from 0.5 mm to 1.5 mm, with a step size of 0.5 mm. The bandwidth and return loss of the antenna are low when W_4 is 0.5 mm and 1.5 mm. However, the reflection coefficient and bandwidth value are improved when W_4 is 1 mm. Therefore, the optimum result is obtained at $W_4 = 1$ mm for the proposed antenna.

4. RESULTS AND DISCUSSIONS

The proposed antenna array has been designed and analyzed with the help of CST microwave studio. A patch antenna array with CSRR has been produced, and the effectiveness of the suggested design is evaluated. the proposed linearly-polarized rectangular microstrip patch antenna array with CSRR is fabricated. The performance of the proposed antenna prototype has been analyzed using the VNA (Vector Network Analyzer). Figs. 5(a) and (b) depict the top and bottom views of the proposed rectangular microstrip patch array antenna with a complementary split ring resonator. Figs. 6(a) and (b) present pho-

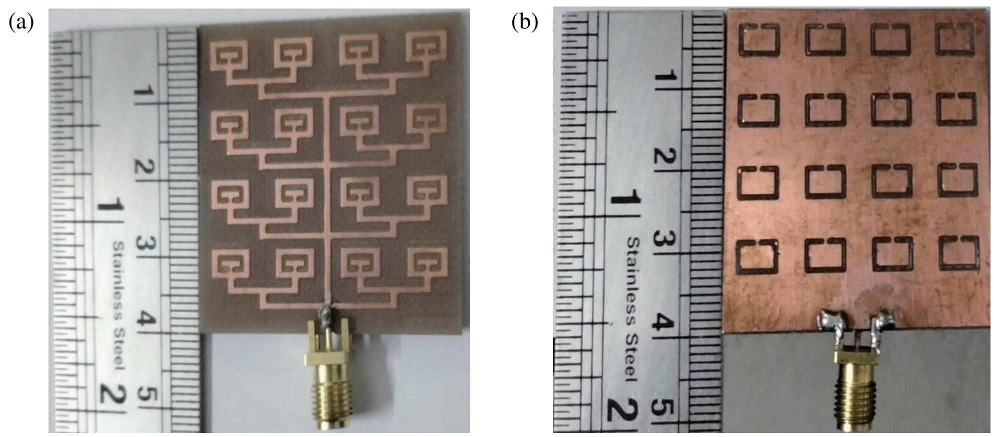

FIGURE 5. Picture of proposed antenna array prototype.

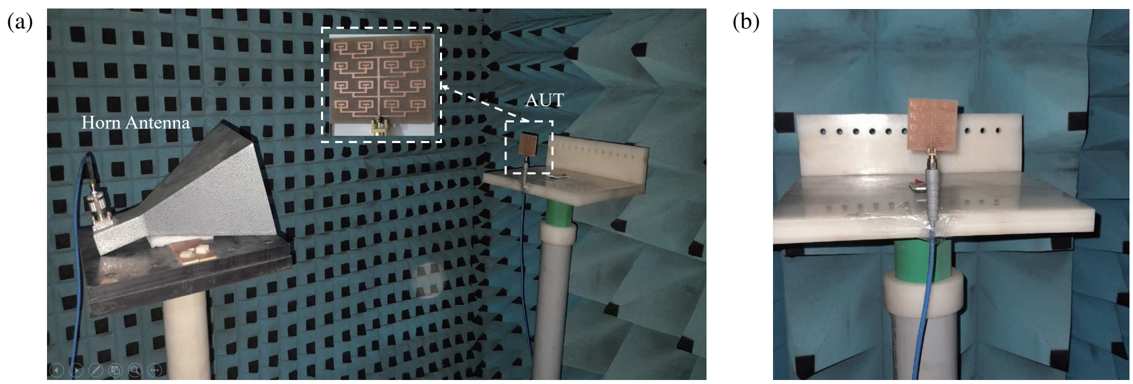

FIGURE 6. Measurement setup of the proposed antenna. (a) AUT measurement, (b) zoom view of AUT.

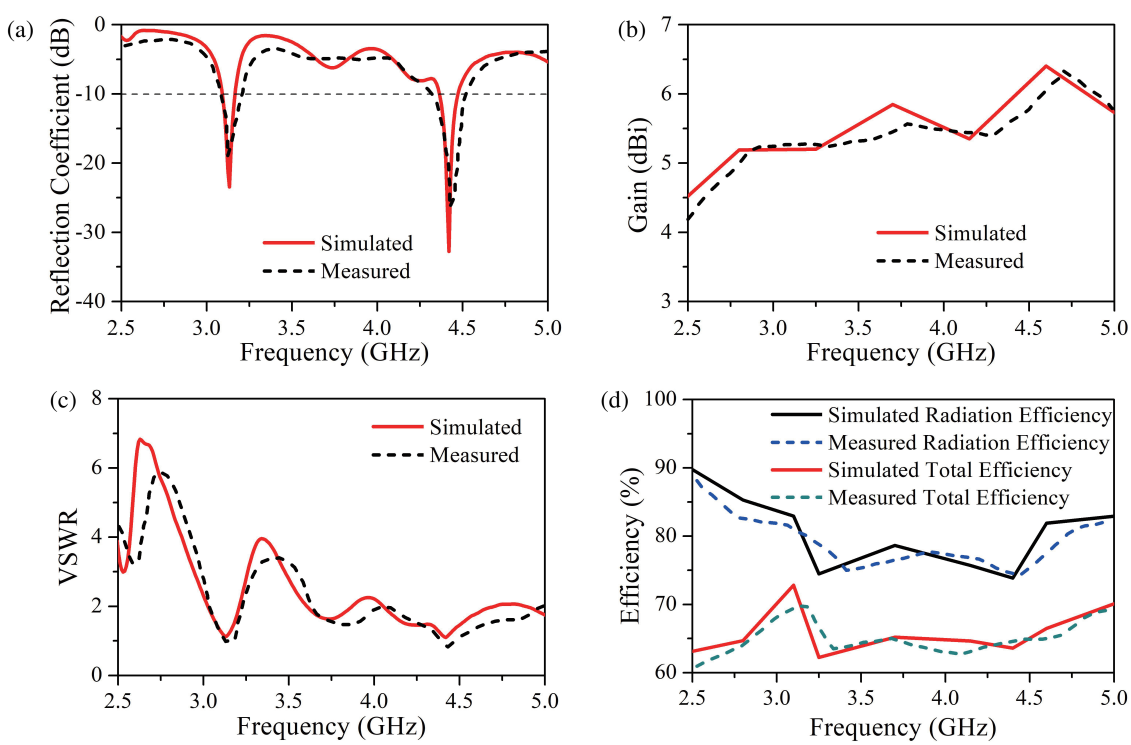

FIGURE 7. Simulated and measured results of the proposed antenna. (a) S_{11}, (b) Gain, (c) VSWR, (d) RE and TE.

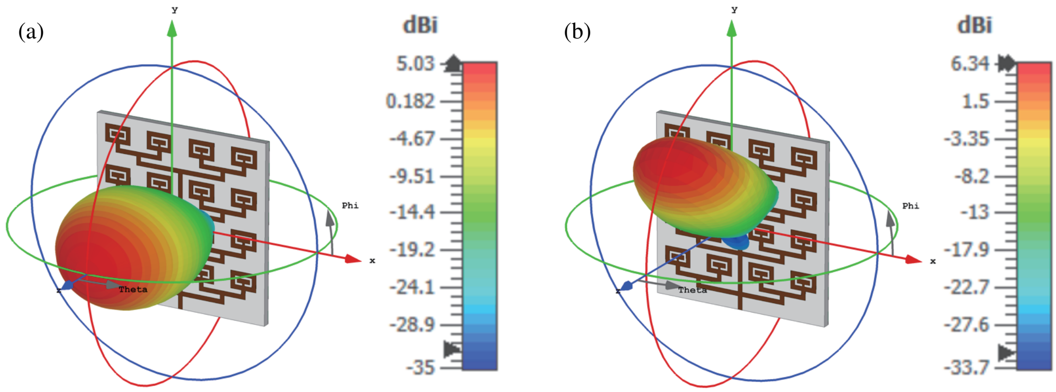

FIGURE 8. Gain plot of proposed antenna at (a) 3.1 GHz (b) 4.4 GHz.

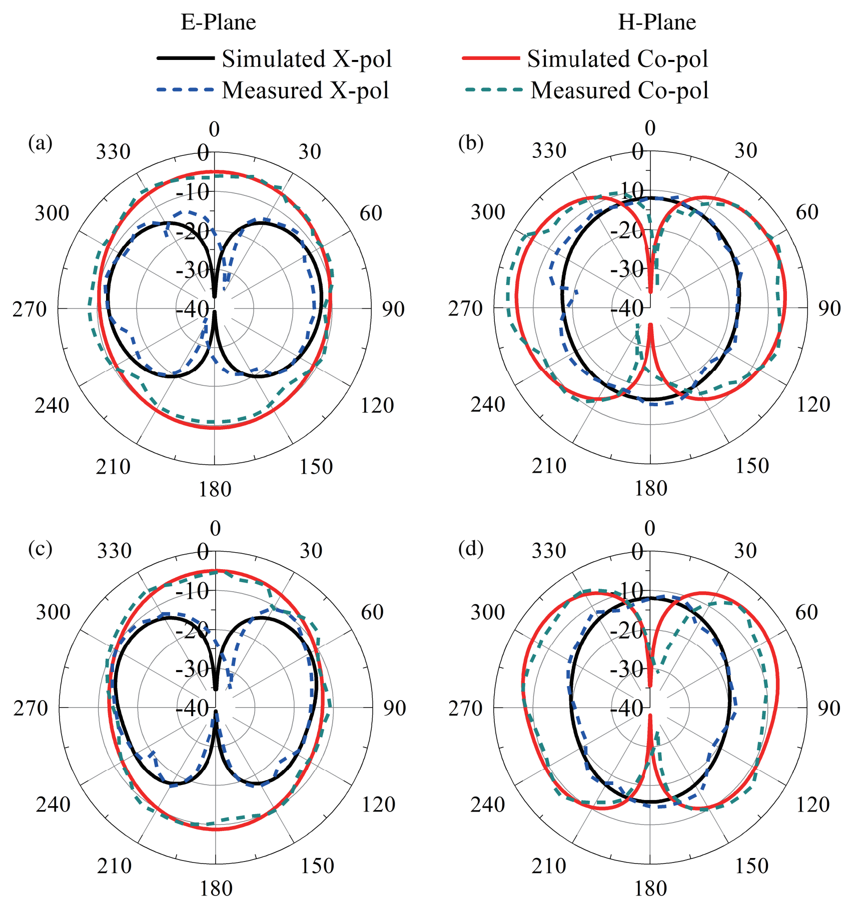

FIGURE 9. Simulated and measured radiation patterns of the array at (a), (b) 3.1 GHz. (c), (d) 4.4 GHz.

tos of the measurement setup in an anechoic chamber. The proposed dual-band antenna is simulated and measured concerning reflection coefficients, and a comparison of results is shown in Fig. 7(a). The results from the simulation and measurements are almost the same.

The small difference between the theoretical and experimental S_{11} values may be because of the VNA cable, fabrication tolerance, or environmental effects. Fig. 7(b) shows the simulated and measured gains vs frequency plot. The simulated and measured voltage standing wave ratios (VSWRs) of the proposed antenna with CSRR are almost equal to the one at resonating frequencies and shown in Fig. 7(c). The simulated and measured radiation efficiencies (REs) and total efficiencies (TEs) of the proposed antenna array results are shown in Fig. 7(d). The proposed antenna's directional three-dimensional (3D) gain characteristics plotted at 3.1 GHz and 4.4 GHz are 5.03 dBi and 6.34 dBi, respectively, as depicted in Figs. 8(a) and (b). Figs. 9(a)–(d) show the simulated and measured co- and cross-polarizations of radiation patterns of the proposed antenna. The radiation pattern plot shows that the maximum radiation occurs

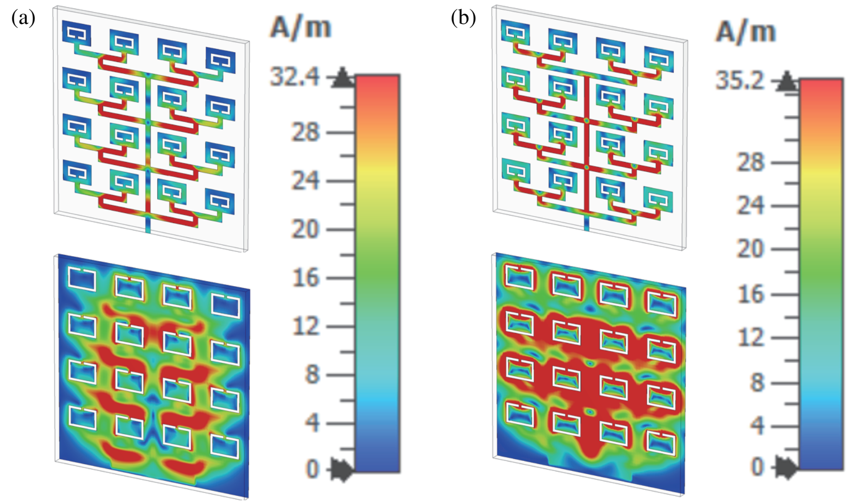

FIGURE 10. Surface current distribution of proposed antenna at (a) 3.1 GHz, (b) 4.4 GHz.

TABLE 3. Comparison study of the proposed antenna with recent published work.

Reference No	Antenna Size (mm^3)	Substrate Material	Resonating Frequency (GHz)	No. of bands	Gain (dBi)	Return loss (dB)
[2]	$50 \times 39 \times 1.6$	FR-4	2.4 3.6	2	6.9 5.8	-23 -26
[3]	$60 \times 200 \times 1.7$	FR-4	2.4	1	6.8	-16
[23]	$669 \times 57 \times 0.9$	Teflon	5.5	1	1.8	-26
[27]	$55.6 \times 50.5 \times 1.6$	FR-4	5.0	1	7.5	-34
[Proposed]	$40 \times 40 \times 1.6$	FR-4	3.1 4.4	2	5.03 6.34	-23 -32

at 0° and 63° in the E and H planes at 3.1 GHz. Similarly, at 0° and 50° maximum radiations for both the E and H planes are observed at 4.4 GHz.

The distributions of the surface currents at 3.1 GHz and 4.4 GHz are illustrated in Figs. 10(a) and (b). The highest current for the suggested antenna is 32.4 A/m, while Figs. 10(a) and (b) display a peak current of 35.2 A/m. Additionally, Table 3 provides a comparison of the proposed cascaded rectangular microstrip patch antenna array with previously published research. From the comparison table, high gain characteristics of the proposed antenna are compared to [23]. The proposed antenna array is more compact than those in [2, 3, 23, 27]. The proposed antenna has good resonance and return loss, which are more suitable for wireless communication applications.

5. CONCLUSION

In this paper, we present the design and analysis of a dual-band cascaded rectangular microstrip patch antenna array with a complementary split ring resonator (CSRR). The antenna array resonates at 3.1 GHz and 4.4 GHz with the reflection coefficients of -23 dB and -32 dB, and impedance bandwidths of 100 MHz (3.06–3.16 GHz) and 110 MHz (4.36–4.47 GHz), respectively. At resonating frequencies, the proposed antenna array has gains of 5.03 dBi and 6.34 dBi. The simulated and measured results of antenna parameters, such as radiation pattern with co-polarization and cross-polarization, reflection coefficient, gain, and surface current distributions are calculated and found to be suitable.

ACKNOWLEDGEMENT

This work has been reinforced by the Science and Engineering Research Board (SERB), New Delhi, India. (Grant No. 1: EEQ/2017/000118, Grant No. 2: SB/FTP/ETA-0179/2014).

REFERENCES

[1] Chen, X., G. Wang, and K. Huang, "A novel wideband and compact microstrip grid array antenna," *IEEE Transactions on Antennas and Propagation*, Vol. 58, No. 2, 596–599, 2010.

[2] Sorathiya, V., A. G. Alharbi, and S. Lavadiya, "Design and investigation of unique shaped low-Profile material-based superlative two-element printed ultrawideband MIMO antenna for Zigbee/WiFi/5G/WiMAX applications," *Alexandria Engineering Journal*, Vol. 64, 813–831, 2023.

[3] Zhang, W., Y. Li, K. Wei, and Z. Zhang, "A high-gain dual-band multibeam antenna system for MIMO Wi-Fi application," *IEEE Transactions on Antennas and Propagation*, Vol. 71, No. 8,

6354–6364, 2023.

[4] Vazquez-Roy, J. L., V. Krozer, and J. Dall, "Wideband dual-polarization microstrip patch antenna array for airborne ice sounder," *IEEE Antennas and Propagation Magazine*, Vol. 54, No. 4, 98–107, 2012.

[5] Xie, J.-J., X.-S. Ren, Y.-Z. Yin, and J. Ren, "Dual-polarised patch antenna with wide bandwidth using electromagnetic feeds," *Electronics Letters*, Vol. 48, No. 22, 1385–1386, 2012.

[6] Trivedi, K. and D. Pujara, "Mutual coupling reduction in wideband tree shaped fractal dielectric resonator antenna array using defected ground structure for MIMO applications," *Microwave and Optical Technology Letters*, Vol. 59, No. 11, 2735–2742, 2017.

[7] Keyrouz, S. and D. Caratelli, "Dielectric resonator antennas: Basic concepts, design guidelines, and recent developments at millimeter-wave frequencies," *International Journal of Antennas and Propagation*, Vol. 2016, No. 1, 6075680, 2016.

[8] Fathipour, M. and L. Asadpor, "Design and fabrication of a multilayer metamaterial antenna with high-gain and good radiation patterns for WiFi and WiMAX applications," *IET Communications*, Vol. 17, No. 4, 448–459, 2023.

[9] Alwareth, H., I. M. Ibrahim, Z. Zakaria, A. J. A. Al-Gburi, S. Ahmed, and Z. A. Nasser, "A wideband high-gain microstrip array antenna integrated with frequency-selective surface for Sub-6 GHz 5G applications," *Micromachines*, Vol. 13, No. 8, 1215, 2022.

[10] Djellid, A., F. Benmeddour, L. Bahri, and A. Ghodbane, "Novel high-gain and compact UWB microstrip antenna for WIFi, WIMAX, WLAN, X band and 5G applications," *Optical and Quantum Electronics*, Vol. 54, No. 7, 441, 2022.

[11] Naik, K. K., "Asymmetric CPW-fed patch antenna with slits at terahertz applications for 6G wireless communications," *Wireless Networks*, Vol. 30, 2343–2351, 2024.

[12] Dadgarpour, A., B. Zarghooni, B. S. Virdee, T. A. Denidni, and A. A. Kishk, "Mutual coupling reduction in dielectric resonator antennas using metasurface shield for 60-GHz MIMO systems," *IEEE Antennas and Wireless Propagation Letters*, Vol. 16, 477–480, 2016.

[13] Naik, K. K., M. Suman, and E. V. K. Rao, "Design of complementary split ring resonators on elliptical patch antenna with enhanced gain for terahertz applications," *Optik*, Vol. 243, 167434, 2021.

[14] Li, B., Y.-Z. Yin, W. Hu, Y. Ding, and Y. Zhao, "Wideband dual-polarized patch antenna with low cross polarization and high isolation," *IEEE Antennas and Wireless Propagation Letters*, Vol. 11, 427–430, 2012.

[15] Kumarnaik, K. and P. A. V. Sri, "Design of hexadecagon circular patch antenna with DGS at Ku band for satellite communications," *Progress In Electromagnetics Research M*, Vol. 63, 163–173, 2018.

[16] Kumar Naik, K. and P. A. V. Sri, "Design of concentric circular ring patch with DGS for dual-band at satellite communication and radar applications," *Wireless Personal Communications*, Vol. 98, 2993–3001, 2018.

[17] Parkash, D. and R. Khanna, "Design and development of CPW-fed microstrip antenna for WLAN/WiMAX applications," *Progress In Electromagnetics Research C*, Vol. 17, 17–27, 2010.

[18] Dattatreya, G. and K. Ketavath, "Tri-band miniaturized elliptical shaped flexible patch antenna for wireless communications at S-band applications," *International Journal of Microwave and Optical Technology*, Vol. 14, No. 1, 37–45, 2019.

[19] Phaneendra, C. N. and K. K. Naik, "Octagonal complementary split ring resonator on rectangular patch MIMO antenna for terahertz applications," *Optik*, Vol. 306, 171808, 2024.

[20] Lee, K. F., S. L. S. Yang, A. A. Kishk, and K. M. Luk, "The versatile U-slot patch antenna," *IEEE Antennas and Propagation Magazine*, Vol. 52, No. 1, 71–88, 2010.

[21] Jafargholi, A., A. Jafargholi, and J. H. Choi, "Mutual coupling reduction in an array of patch antennas using CLL metamaterial superstrate for MIMO applications," *IEEE Transactions on Antennas and Propagation*, Vol. 67, No. 1, 179–189, Jan. 2019.

[22] Naik, K. K., "Improvement of wider bandwidth using dual e–shaped antenna for wireless communications in 5G applications," *Analog Integrated Circuits and Signal Processing*, Vol. 109, No. 1, 93–101, 2021.

[23] Zhao, X.-L., J. Jin, J.-C. Cheng, and L.-G. Liang, "A wideband dual-polarized array antenna with conical elements for Wi-Fi/WiMAX application," *IEEE Antennas and Wireless Propagation Letters*, Vol. 13, 1609–1612, 2014.

[24] Wang, B., Z. Zhao, K. Sun, C. Du, X. Yang, and D. Yang, "Wideband series-fed microstrip patch antenna array with flat gain based on magnetic current feeding technology," *IEEE Antennas and Wireless Propagation Letters*, Vol. 22, No. 4, 834–838, Apr. 2023.

[25] Ketavath, K. N., "Enhancement of gain with coplanar concentric ring patch antenna," *Wireless Personal Communications*, Vol. 108, No. 3, 1447–1457, 2019.

[26] Iqbal, Z., T. Mitha, and M. Pour, "A self-nulling single-layer dual-mode microstrip patch antenna for grating lobe reduction," *IEEE Antennas and Wireless Propagation Letters*, Vol. 19, No. 9, 1506–1510, 2020.

[27] Li, W., Y. M. Wang, Y. Hei, B. Li, and X. Shi, "A compact low-profile reconfigurable metasurface antenna with polarization and pattern diversities," *IEEE Antennas and Wireless Propagation Letters*, Vol. 20, No. 7, 1170–1174, 2021.

[28] Kannan, T., F. Taher, M. F. A. Sree, and S. Lavadiya, "Compact and high gain cup-shaped 4-Port MIMO antenna using low profile material for the sub-6 GHz, IoT and military applications," *Physica Scripta*, Vol. 99, No. 5, 055501, 2024.

[29] Saxena, G., P. Jain, and Y. K. Awasthi, "High diversity gain super-wideband single band-notch MIMO antenna for multiple wireless applications," *IET Microwaves, Antennas & Propagation*, Vol. 14, No. 1, 109–119, 2020.

[30] Phaneendra, C. N. and K. K. Naik, "Inset-fed octagonal-shaped quad-port MIMO patch antenna for UWB applications," *Wireless Personal Communications*, Vol. 138, 1311–1327, 2024.

[31] Ketavath, K. N., "Dual-band crescent-shaped slot patch antenna for wireless communications and IoT applications," *Microwave and Optical Technology Letters*, Vol. 65, No. 8, 2392–2398, 2023.

[32] Roy, B. and Y. Venkata Lakshmaiah, "Super wideband with band rejection characteristics circular patch monopole antenna for 5G and beyond," *Physica Scripta*, Vol. 98, No. 9, 095513, 2023.

[33] Sailaja, B. V. S. and K. K. Naik, "CPW-fed elliptical shaped patch antenna with RF switches for wireless applications," *Microelectronics Journal*, Vol. 111, 105019, 2021.

[34] Islam, S., B. Halder, and A. R. Ali, "Optical and rogue type soliton solutions of the (2 + 1) dimensional nonlinear heisenberg ferromagnetic spin chains equation," *Scientific Reports*, Vol. 13, No. 1, 9906, 2023.

[35] Krishna, O. and K. K. Naik, "Analysis of triangular antenna with two annular rings for multi-band applications," *Journal of Critical Reviews*, Vol. 7, No. 4, 189–191, 2020.

[36] Refaie Ali, A., M. N. Alam, and M. W. Parven, "Unveiling optical soliton solutions and bifurcation analysis in the space–time fractional Fokas–Lenells equation via SSE approach," *Scientific*

Reports, Vol. 14, No. 1, 2000, 2024.

[37] Sailaja, B. V. S. and K. K. Naik, "Design and analysis of serpentine meander asymmetric cantilever RF-MEMS shunt capacitive switch," *Analog Integrated Circuits and Signal Processing*, Vol. 102, 593–603, 2020.

[38] Refaie Ali, A., H. O. Roshid, S. Islam, and A. Khatun, "Analyzing bifurcation, stability, and wave solutions in nonlinear telecommunications models using transmission lines, Hamiltonian and Jacobian techniques," *Scientific Reports*, Vol. 14, No. 1, 15282, 2024.

[39] Khan, M. H., S. Islam, and A. R. Ali, "Certain results associated with lump and periodic-soliton solutions for (2 + 1)-D Calogero–Bogoyavlenskii–Schiff equation," *Journal of Applied Mathematics and Statistical Analysis*, Vol. 4, No. 2, 43–57, 2023.

[40] Naik, K. K., "Asymmetric CPW-fed SRR patch antenna for WLAN/WiMAX applications," *AEU — International Journal of Electronics and Communications*, Vol. 93, 103–108, 2018.

[41] Yang, X.-J., A. A. Alsolami, and A. R. Ali, "An even entire function of order one is a special solution for a classical wave equation in one-dimensional space," *Thermal Science*, Vol. 27, No. 1, 491–495, 2023.

[42] Khan, M., F. Mahmood, M. Ali, Y. Wang, A. R. Ali, and A. H. Majeed, "Synthesis of hierarchical porous carbon scaffold derived from red kidney bean peels for advanced Li–Se and Na–Se batteries," *Scientific Reports*, Vol. 14, No. 1, 17749, 2024.

[43] CST Microwave Studio, 2022, http://www.cst.com.